

Cadaveric Study of Anterior Cruciate Ligament Failure Patterns Under Uniaxial Tension Along the Ligament

Nikolaos K. Paschos, M.D., Dimitrios Gartzonikas, M.D., Nektaria-Marianthi Barkoula, Ph.D., Constantina Moraiti, M.D., Alkis Paipetis, Ph.D., Theodore E. Matikas, Ph.D., and Anastasios D. Georgoulis, M.D.

Purpose: The purpose of our study was to clarify the events that take place during anterior cruciate ligament (ACL) failure, focusing on the behavior of the ACL as a composition of multiple fibers, during uniaxial tension along the ligament. **Methods:** Ten fresh-frozen human cadaveric knee specimens were fixed in an Instron machine (Instron, Norwood, MA), and load was applied parallel to the ACL axis. Two cameras were used to detect the failure mode of the ACL and its different groups of fibers. The distinct bundles of fibers were marked in each specimen before testing. The macroscopic findings during the experiment were used for comparison with the biomechanical results. **Results:** The ACL showed a non-monotonic response during testing. The load-elongation curve showed a plateau or a second peak after the initial drop in load. Macroscopically, some fibers were failing initially, whereas the intact fibers had a remaining load potential. In our setting, 3 different failure patterns were recognized, specifically, a midsubstance tear of the anteromedial or the posterolateral bundle with a subsequent failure of the intact bundle or an initial avulsion of the anteromedial attachment. Analysis of the video frames showed a direct connection between the failure patterns in the load-elongation curves and the macroscopic sequence of events during ACL failure. **Conclusions:** The ACL ligament acts as a multifiber construction. In our setting, rupture follows 3 specific patterns where a complete or partial tear of the fiber bundles occurs first and the remaining intact fiber bundles have a potential load resistance. **Clinical Relevance:** Our study allows a better understanding of the mechanical properties of the ACL. An update on the biomechanics of ACL failure during uniaxial tension after the “double-bundle revolution” could provide data helpful for ACL reconstruction.

Since the first report of varying tightness and laxity during knee flexion for the different subdivisions of the anterior cruciate ligament (ACL) in 1836,¹ it has been well established that there are distinct functional roles of the different fibers. Several authors

have evaluated the anatomy of the ACL concerning the different bundles suggested.²⁻⁴ Two main bundles have been depicted: anteromedial (AM) and posterolateral (PL).² The interest of the orthopaedic community regarding ACL biomechanics has increased based on indications that each bundle has a different role in knee joint stability and overall knee function.⁵

Increased interest related to the distinct role of the AM and PL bundles in anterior tibial translation (ATT) and internal rotation (IR) of the knee has evolved.⁶ Despite the fact that the role of the ACL in restraining ATT and IR was highlighted early,⁷ it was only recently that in vitro biomechanical studies suggested the separate action of the PL bundle in stabilizing the knee against ATT in IR.^{8,9} In vivo studies confirmed the insufficiency of the AM bundle recon-

From the Orthopaedic Sports Medicine Center of Ioannina, Department of Orthopaedic Surgery (N.K.P., D.G., C.M., A.D.G.), and Department of Materials Science and Engineering (N-M.B., A.P., T.E.M.), University of Ioannina, Ioannina, Greece.

The authors report no conflict of interest.

Received June 1, 2009; accepted December 4, 2009.

Address correspondence and reprint requests to Anastasios D. Georgoulis, M.D., G. Papandreou 2, PO Box 1330, 45110 Ioannina, Greece. E-mail: oaki@cc.uoi.gr

© 2010 by the Arthroscopy Association of North America

0749-8063/9329/\$36.00

doi:10.1016/j.arthro.2009.12.013

struction in rotational instability.^{10,11} Recently, however, only a minor contribution of the PL bundle in anteroposterior laxity was proposed.¹²

In addition, the effect of different knee joint angles on the biomechanics of the AM and PL bundles has been highlighted by some authors.^{8,13,14} According to their results, the AM bundle was carrying increasing in situ force with increasing knee flexion up to 60° of flexion. At knee flexion at 90° or more, the in situ force in the AM bundle was slightly decreasing. The opposite was observed in the PL bundle, where the in situ force was decreasing with increasing flexion. The AM and PL bundles had similar in situ force distributions at 15° of knee flexion.⁸

Although the biomechanics of ACL failure have been examined in various cadaveric models, the incidents occurring during ACL rupture with regard to the ACL's different fiber bundles have not been emphasized.^{5,15-17} Noyes et al.¹⁵⁻¹⁷ reported their considerations on ACL failure in animal cadaveric knees. The specimens were placed with the knee joint positioned at 45° of flexion and were loaded in tension to failure.^{15,16} A load-versus-time diagram for the behavior of the ACL during rupture was presented, where different strain rates resulted in different failure modes.^{15,16} The effects of age and orientation to the structural properties of the ACL have also been highlighted.⁵ In these studies tensile load was applied along the axis of the ACL with a strain rate ranging from 0.084 to 8.46 mm/s.^{5,15-17} This scenario does not correspond to the force acting on the ACL during a typical knee trauma, which is represented by the anterior-drawer scenario. Different macroscopic modes of failure have been depicted.^{5,15-17} These ruptures mainly concerned the substance of the ACL.^{5,15-17} Frequently, the failure consisted of an avulsion of the ligament at the ligament-bone

interface.^{5,15-17} Several combinations have been reported.^{5,15-17} Recently, a clinical study emphasized the potential role of the different bundles in partial ACL rupture.¹⁸

Thus the purpose of our study was to investigate the events that take place during ACL failure. We aimed to evaluate the behavior of the ACL as a composition of multiple fibers, during uniaxial tension along the ligament. We hypothesized that the ACL is not an isometric structure but, rather, that it is composed of different functional groups of fibers. Furthermore, we hypothesized that the rupture pattern of the ACL during uniaxial tension along the ligament is related to the behavior of its different groups of fiber bundles, namely the AM and PL bundles.

METHODS

Ten fresh-frozen human cadaveric knee specimens were used in this study. Institutional review board approval was obtained from our institution for the use of the specimens. The mean age of the donors was 74 years (range, 44 to 88 years). There were 5 male donors and 5 female donors. All details on the demographics of the tested specimens are presented in Table 1. Knees that had evidence of previous operative treatment were excluded. Specimens were wrapped in saline solution-soaked gauze, double bagged in sealed polyethylene bags, and stored at -20°C until 24 hours before preparation and/or testing, at which time they were thawed at room temperature.¹⁹ During unfreezing and preparation, the specimens were kept moist with saline solution-soaked gauze. All cadaveric specimens were assessed physically for stability, and the joint surfaces were inspected visually to ensure that no gross abnormalities were present. In preparation for

TABLE 1. Demographics, Dimensions, Maximum Load, Elongation at Break, Stiffness, and Young's Modulus of Tested ACL Specimens

	Specimen No.										Mean	SD
	1	2	3	4	5	6	7	8	9	10		
Age (yr)	52	82	63	78	44	71	88	83	87	88	73.6	15.8
Gender	M	F	M	F	M	M	F	F	M	F		
Length (mm)	22	20	20	16	29	31	19	18	22	20	21.7	4.7
Diameter (mm)	7	8	7	6	7	9	12	12	13	10	9.1	2.5
Maximum load (N)	637	169	741	326	838	149	210	248	368	315	400.1	248.0
Elongation at break* (mm)	16.1	18.5	29.2	21.6	26.2	24.1	29.4	29.9	29.2	25.8	23.3	8.8
Stiffness (N/mm)	61	33	65	44	101	35	42	38	90	63	57.2	23.5
Young's modulus (MPa)	35	13	34	25	76	17	7	6	15	16	24.4	20.7

*Ninety percent drop in peak load.

testing, all soft tissues were carefully removed except for the ACL. The ACL was considered to have a cylindrical shape with a circular cross section. To measure the mean length and diameter of the ACL, each specimen was positioned on a horizontal table in full extension. The diameter of the ACL was measured at least at 3 points along the free length of the ACL (close to the femur, close to the tibia, and in the middle of the ACL specimen), and a mean value was calculated. The maximum length between the femur and tibia was determined in 3 positions (anterior side, posterior side, and lateral side of ACL), and a mean value was calculated. All dimensions were measured with a digital caliper and are shown in Table 1.

Specimen Fixation

A custom clamping device was designed and manufactured (Fig 1) to ensure reproducible placement of the tibial and femoral components of the specimens.

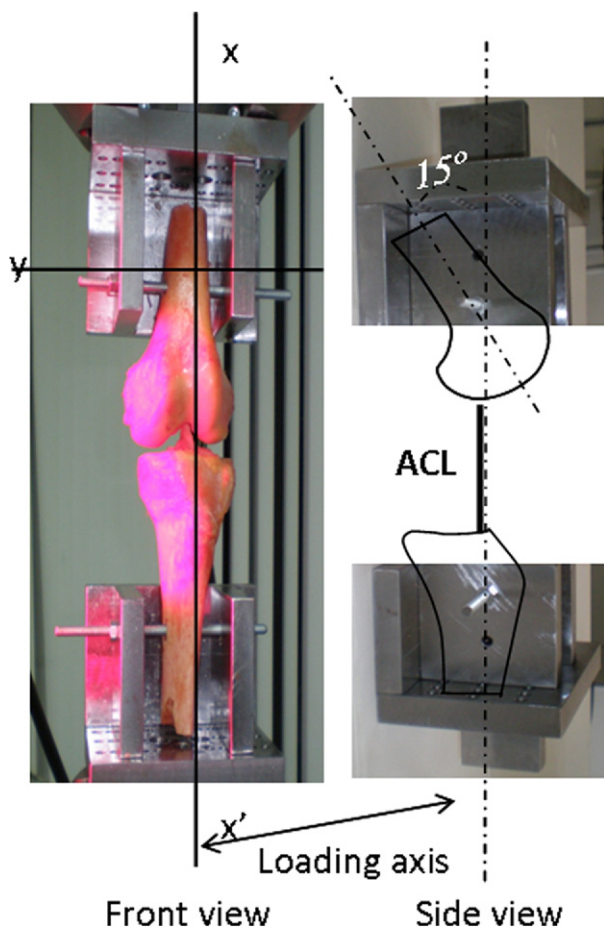


FIGURE 1. Front and side view of custom clamping device.

The clamping device consisted of 2 clamps, 1 for the femur and 1 for the tibia. In this study 1 set of transverse holes was drilled in the femur and 1 in the tibia. The knee angle was measured with a digital goniometer, and each knee was placed in 15° of flexion. The axis of the femur and tibia was placed in accordance with the ACL axis to avoid varus/valgus and torsion rotation variations. A set of pins was placed through the femur and tibia to secure the femur and tibia, avoiding horizontal and vertical movement. Two custom-made, square-shaped nuts were used as fasteners to secure the position and avoid rotation of the femur and tibia around the pins. The current settings were selected to serve as a model to examine the behavior of the different fiber portions in a specific loading situation, where the tension is applied directly to the ligament and equally among the ACL's different bundles.

Testing

The biomechanical tests were conducted on an Instron 8801 servohydraulic machine (Instron, Norwood, MA) with a maximum load ± 100 kN. For this study, a 5-kN load cell was used. After mounting of the specimen in the custom clamping device, the clamps were attached, with one side (femur) attached to the load cell of the testing machine and the other side (tibia) attached to the actuator of the materials testing machine. The specimen was loaded from the relaxed position up to failure at a displacement rate of 1.5 mm/s. No pre-tensioning was applied to the specimen, because the fixation of the specimen in the clamps allowed control of the alignment of the specimen with the loading axis. This resulted in a delay in load uptake, as recorded in the load-elongation curves.

A non-contact video extensometer, supplied by Instron, was used to monitor the displacement. Its use allowed accurate measurement of ACL elongation, because application of traditional contact extensometers, such as mechanical clip-on extensometers or strain gauges, is not appropriate when one is examining soft-tissue specimens such as the ACL. The video extensometer consisted of a high-resolution digital camera and advanced real-time image processing. Elongation was measured by tracking contrasting gauge marks placed on the specimen. The gauge marks were applied on the free length of the ACL specimen, and their initial distance was measured by the extensometer software before testing. Failure was defined as the complete rupture of the ligament or when the load on the ligament was below 90% of its

maximum value (i.e., the ligament could carry only 10% of its maximum load). The previously described procedure allowed for the recording of the specimen's load-elongation curves. The maximum load to failure was defined as the point where a marked load decrease was observed in the load-elongation curve. The stiffness of the testing sample was determined by calculating the gradient of the linear portion of the load-elongation curve. Stiffness (k) is defined as follows:

$$k = \Delta F / \Delta L$$

where ΔF indicates load (in newtons) and ΔL indicates elongation (in meters).

The modulus of elasticity, or Young's modulus, was calculated from the gradient of the linear portion of the stress-strain curve by dividing the change in stress ($\Delta\sigma$) (in newtons) by the change in strain ($\Delta\varepsilon$) (in square millimeters). Young's modulus (E) (in megapascals) is defined as follows:

$$E = \Delta\sigma / \Delta\varepsilon$$

Stress (σ) (in megapascals) was calculated as follows:

$$\sigma = F/A$$

where F indicates load (in newtons) and A indicates cross-sectional area (in square millimeters).

Strain (ε) was calculated as follows:

$$\varepsilon = \Delta L/L$$

where ΔL indicates elongation and L indicates initial length.

Three orthopaedic surgeons with experience in arthroscopic reconstruction of the ACL evaluated the specimens separately. All surgeons were asked to distinguish the 2 bundles of the ACL on the specimens both after soft-tissue removal and after fixation in the Instron machine. Each surgeon marked the different bundles before testing based on their femoral and tibial attachments.² A separation of the bundles by blunt dissection could potentially harm the ligament and alter the results of testing; therefore it was avoided.

With the use of 2 high-resolution high-speed digital cameras (frame rate, 200 Hz), one monitoring the experimental process from the anterior aspect of the knee joint and the other filming the posterior surface, each surgeon was asked to describe the macroscopic response of the ACL during testing. Each surgeon investigated the macroscopic responses from recorded tapes and had the opportunity to watch the sequences repeatedly. The surgeons were blinded to each other's results. They documented whether the rupture was a

midsubstance tear of the ligament or an avulsion from the tibial or femoral attachment of the ligament. Furthermore, they indicated whether the tear involved only part of the AM or PL bundle or whether it involved all the fibers comprising each bundle. The sequence of events was also reported. Subsequently, each surgeon, blinded to each other, performed an analysis of the video frames in relation to the changes in the load-elongation curves to assess the behavior of the different groups of fibers of the ACL during tension and rupture.

RESULTS

Figure 2 shows the load-elongation response of the 10 ACL specimens tested. The results are plotted in separate graphs to maximize the resolution of each curve. The maximum load, elongation at break (or 90% drop in peak load), stiffness, and Young's modulus of each of the 10 ACL specimens are shown in Table 1. The different ACL specimens showed maximum load values varying between 149 and 838 N and maximum elongation values between 16.1 and 29.9 mm. The stiffness values varied between 33 and 101 N/mm, whereas the Young's modulus values ranged between 6 and 76 N/mm². We observed that younger specimens had a higher load at failure and a higher modulus of elasticity. Similar trends were observed in the stiffness values, although in 2 cases (specimens 9 and 10), quite high stiffness values did not coincide with a high modulus of elasticity or young donors.

All 10 ACL specimens responded in a ductile failure manner, that is, they continued to deform after the maximum load was achieved and failed after extended plastic deformation occurred. No specimen showed a monotonic response; thus in all cases the response of the ACL was not monotonic. Three patterns were observed in the load-elongation curves. In the first pattern (A), the initial drop in load after reaching its maximum value was followed by a plateau in the load-elongation curve (specimens 1, 2, 3, and 7). In the second pattern (B), after the first peak, a second peak in load was noted as the elongation increased (specimens 4, 8, and 10). In the third pattern (C), both a second peak and a plateau (specimens 5, 6, and 9) were observed. It is interesting to note that the load in some cases reached values comparable to its initial maximum (specimens 4, 5, 6, 8, and 10) (Fig 2).

The macroscopic behavior of the ACL concerning the different groups of fibers was documented by the orthopaedic surgeons independently. The description of the events for each specimen matched completely

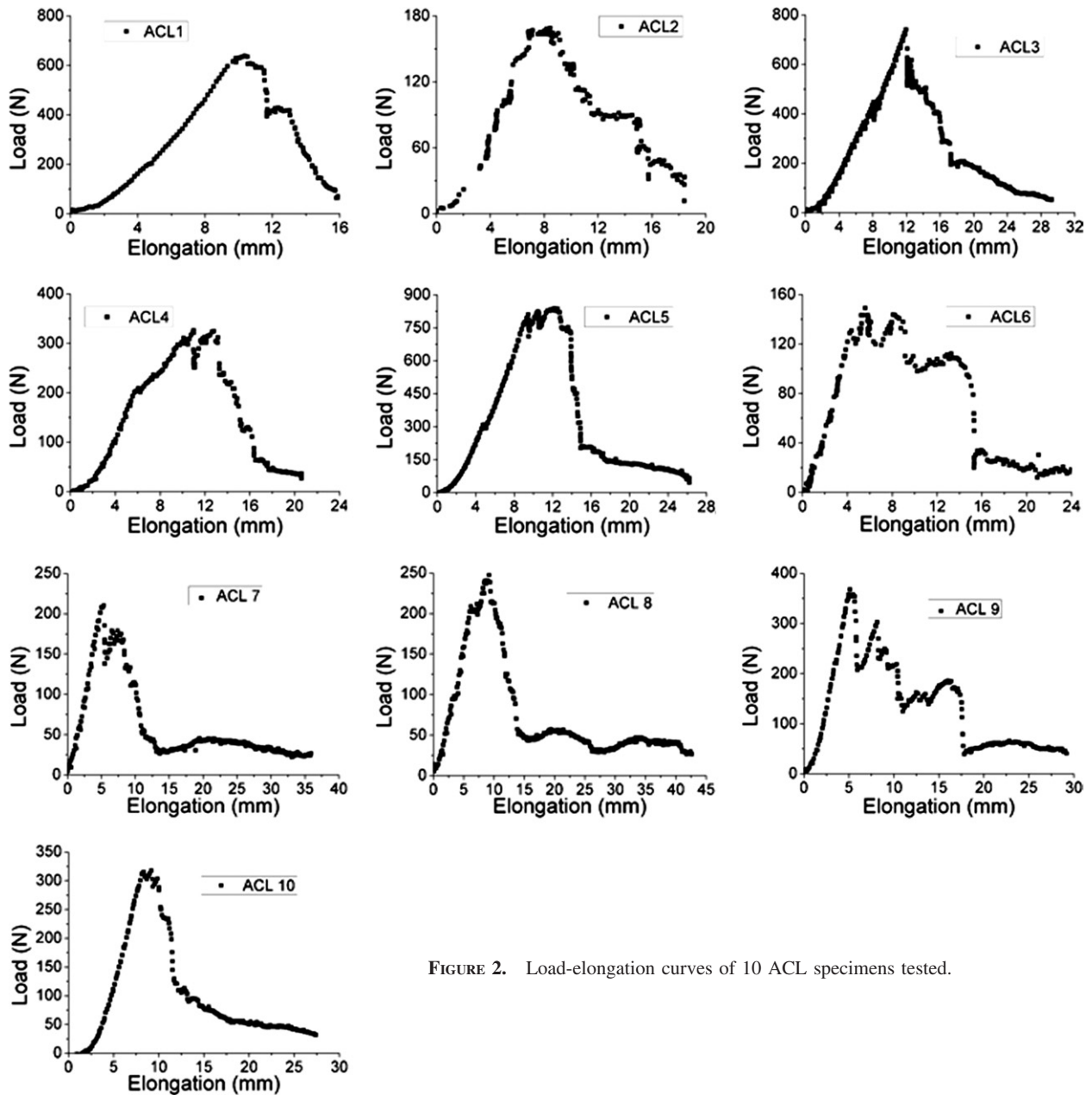


FIGURE 2. Load-elongation curves of 10 ACL specimens tested.

between all 3 surgeons. Three different patterns of ACL failure were described. The first pattern involved a midsubstance tear of the AM bundle followed by a subsequent tear of the PL bundle (specimens 1, 2, 3, and 7). The second pattern involved a midsubstance tear of the PL bundle first, followed by a tear of the AM bundle (specimens 4, 8, and 10). The third pattern involved an avulsion of the tibial attachment of part of the fibers of the AM bundle, followed by a midsubstance tear of the PL bundle, and lastly, a midsub-

stance tear of the remaining fibers of the AM bundle (specimens 5, 6, and 9).

The analysis of the video frames during testing showed a direct connection between the aforementioned failure patterns (A, B, and C) and the sequence of events. Examples of the 3 patterns, namely A, B, and C, and their correlation to the macroscopic sequence of events are depicted in Figs 3, 4, and 5 in specimens 7, 8, and 9, respectively. As shown in Fig 3, the tear of the AM bundle coincided with the initial

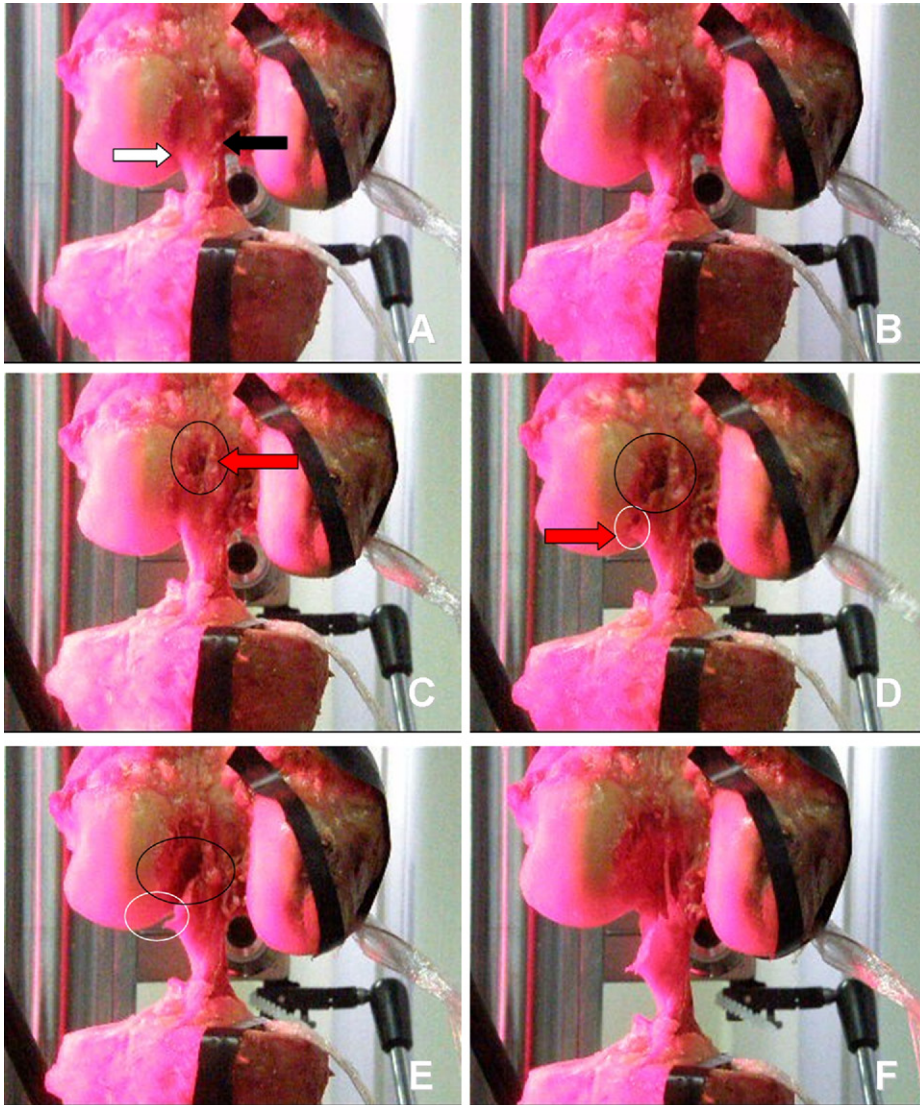
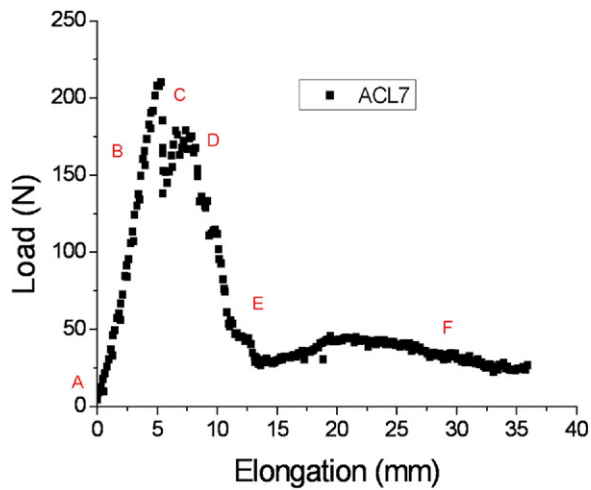


FIGURE 3. Images of ACL failure pattern A (specimen 7). (A) AM (black arrow) and PL (white arrow) bundles of ACL before loading. (B) The ACL deforms with load application. (C) Initiation of failure of some of the AM fibers (black oval) close to their femoral attachment (red arrow). (D) Whereas the tear of the fibers belonging to the AM bundle progresses laterally (black circle), some of the fibers of the PL bundle (white oval) begin to tear (red arrow). (E) Both AM fibers (black oval) and PL fibers (white oval) are significantly torn. (F) Complete failure of the ACL without load ability. Graph: Load-elongation curve indicating failure pattern A of the ACL. A through F correspond to the events during ACL failure as shown in the photographs.



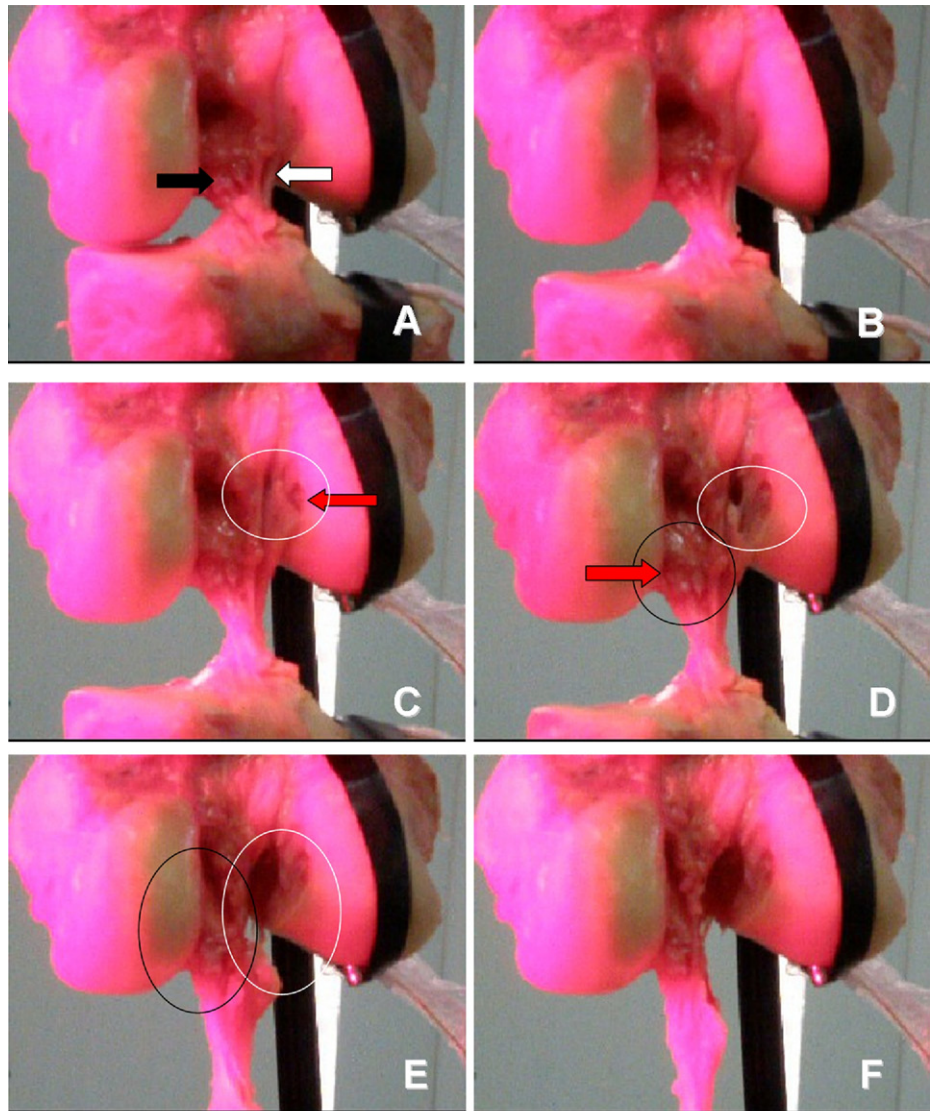
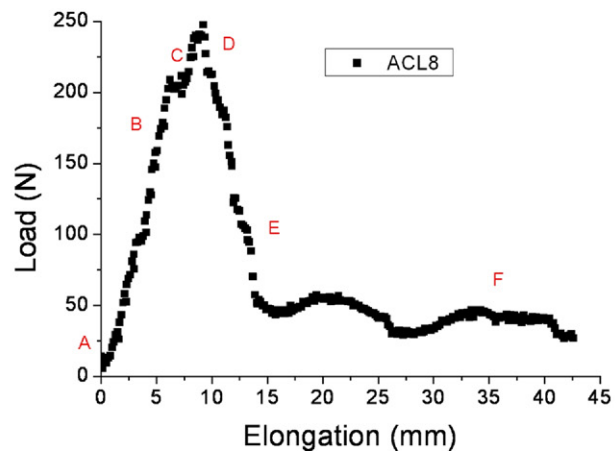


FIGURE 4. Images of ACL failure pattern B (specimen 8). (A) AM (black arrow) and PL (white arrow) bundles of ACL before loading. (B) The ACL deforms with load application. (C) Initiation of failure of PL bundle (white oval) close to femoral attachment (red arrow). (D) The failure of the PL continues (white oval), whereas there are some tears (red arrow) visible in the AM bundle (black circle). (E) Both AM fibers (black oval) and PL fibers (white oval) are significantly torn. (F) Complete failure of ACL without load ability. Graph: Load-elongation curve indicating failure pattern B of ACL. A through F correspond to the events during ACL failure as shown in the photographs.



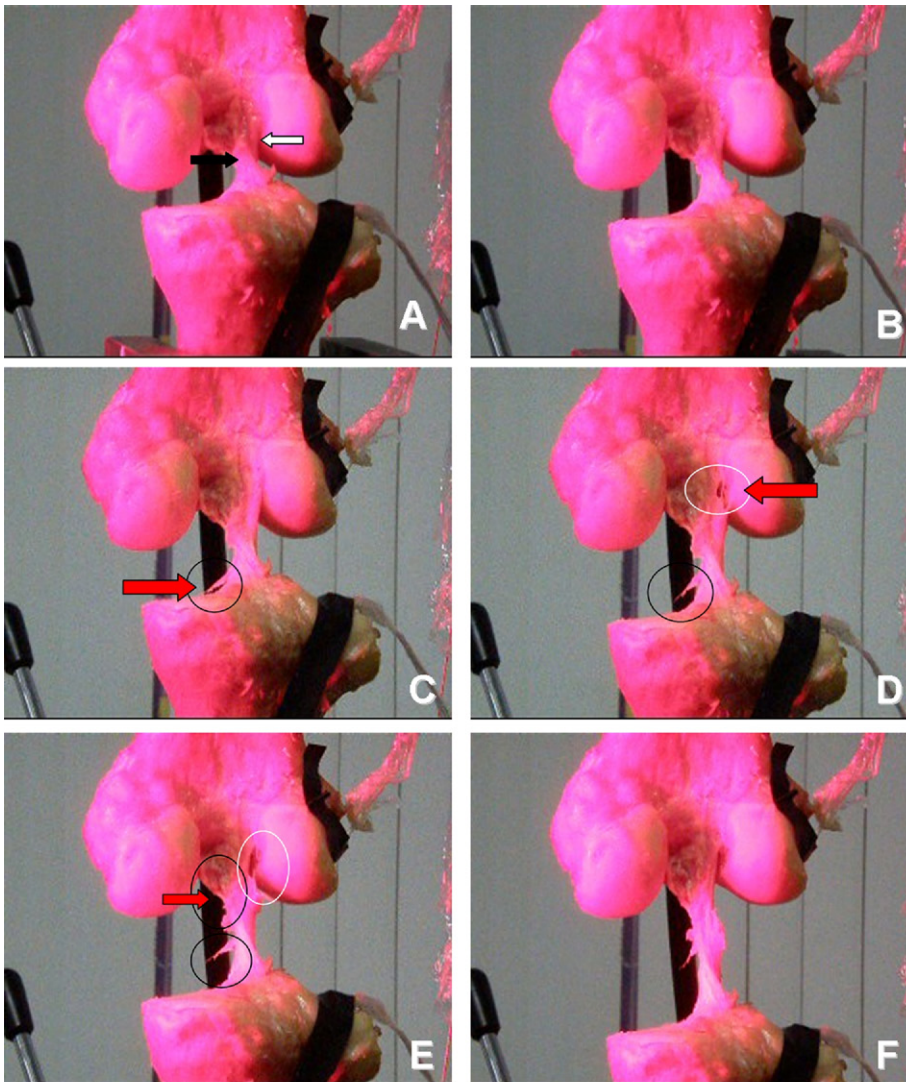
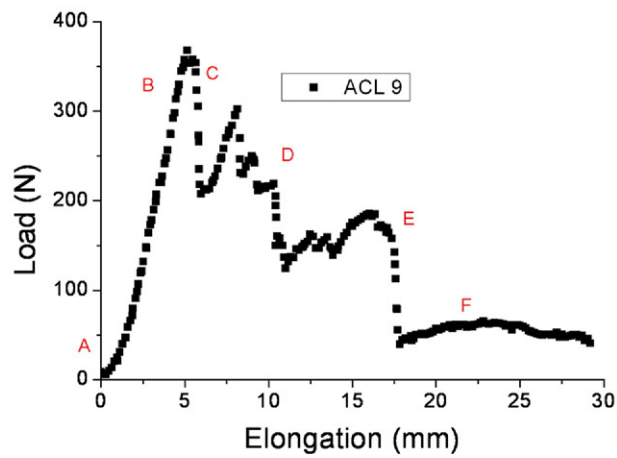


FIGURE 5. Images of ACL failure pattern C (specimen 9). (A) AM (black arrow) and PL (white arrow) bundles of ACL before load application. (B) The ACL deforms with load application. (C) An avulsion of the tibial attachment of part of the fibers (red arrow) of the AM bundle (black circle) is the initial failure marked. (D) Some fibers of the PL bundle (white oval) begin to fail (red arrow). (E) Whereas the tear at the tibial attachment of the AM bundle and the tear of the PL fibers continue to evolve, a midsubstance tear (red arrow) of the intact AM fibers (black oval) initiates. (F) Complete failure of the ACL without load ability. Graph: Load-elongation curve indicating failure pattern C of ACL. A through F correspond to the events during ACL failure as shown in the photographs.



decrease in the load-elongation curve. The load-carrying ability of the PL band is depicted by the subsequent plateau in the load-elongation curve. The second failure pattern (B) is shown in Fig 4. The ligamentous tear of the PL band was shown by the declining part of the load-elongation curve. The load-carrying ability of the AM bundle was depicted by a second peak in the curve. As shown in Fig 5, in the third pattern (C) the tibial avulsion occurring in some AM fibers was shown by the initial decrease in the load-elongation curve. The load-carrying ability of the PL bundle and that of the remaining AM fibers coincided with a second peak and a plateau in the load-elongation curve, respectively.

DISCUSSION

Our hypothesis that the ACL acts as a multifiber construction rather than a single-component structure during its elongation and its consecutive rupture was confirmed. Furthermore, the rupture pattern of the ACL during uniaxial tension along the ligament was related to the behavior of its different groups of fiber bundles.

In our study all ACL specimens showed a non-monotonic response. If the ACL was behaving as 1 single fiber, then the rupture would translate into complete monotonic failure of the specimen. The fact that load initially drops and then peaks up again leads to the conclusion that the ACL acts as a multifiber construction. The 3 different failure patterns shown in the load-elongation curve and their direct relation to the macroscopic sequence of events during ACL failure confirmed our second hypothesis, because they suggest that the rupture of the different groups of fibers of the ACL in a separate time mode could be responsible for the final pattern.

Our results are in line with previously reported results. The diagram pattern found in our study shows similarities to the oscillographs presented by Noyes et al.¹⁵⁻¹⁷ In these studies the decreased curves depicted were justified as successive failures that appear in an unpredictable fashion.¹⁵ However, the differences in the diagram presented in our study and that of Noyes et al.¹⁵ could be explained by the fact that our study used cadaveric human knees whereas the results from their study were based on an animal model.

The macroscopic failure patterns shown in our study have also been reported in previous studies.^{20,21} A midsubstance pull-apart failure of the ligament and an avulsion of the ligament at the insertion site to the femur or the tibia are the most commonly described

ACL failure modes. A minor to major avulsion fracture of bone at the insertion site has also been reported. More rarely, a failure through the fibrocartilaginous attachment site at the bone-ligament interface has been described.^{21,22}

According to the obtained descriptions, some fibers were failing initially, whereas the intact fibers had a remaining load potential. This was illustrated either by a plateau in the diagram or by a second peak. Despite the fact that the AM and PL bundles acted as separate structures, the rupture of the one structure allowed the other to operate under load; therefore, we presume that the different bundles act synergistically with each other. Further tensioning of the ACL results in rupture of the intact fibers and a consequent inability to withstand load. On the basis of these observations, we presume that the setting described previously, with incomplete failure of the ligament, represents the previously described condition of partial rupture of the ACL. Although partial rupture of the ACL has been documented frequently in the literature, either as an arthroscopic finding^{23,24} or based on a magnetic resonance imaging (MRI) reading,^{25,26} it was only recently that the rupture pattern related to the 2 functional bundles was evaluated in a clinical study.¹⁸ A partial ACL rupture in 25% of patients undergoing ACL reconstruction based on clinical criteria was reported.¹⁸ The failure pattern of the ACL was different among these patients, with 44% of the AM and PL bundles not being ruptured at the same level. Furthermore, the PL bundle was intact in 12% of the patients. These results can imply a different mechanism of failure of the 2 bundles.¹⁸ Although the role of MRI in the diagnosis of ACL failure is well established,²⁷ it was only recently that different ACL rupture patterns were shown by use of a 3-T MRI technique.²⁸

Although certain patterns of failure were detected concerning the role of the different groups of fiber bundles, significant differences in maximum load and elongation values were obtained between the different specimens. Furthermore, as described in the "Results" section, we observed that specimens aged over 65 years had a lower maximum load and lower modulus of elasticity, which is in accordance with previous results on the effect of age on the tensile properties of the ACL.^{5,17} Data on linear stiffness, energy absorption, and ultimate load for the human femur-ACL-tibia complex have shown the contribution of age and angular orientation of the complex to its mechanical performance.⁵ It should be noted, however, that there was no direct correlation between these parameters

and the observed failure patterns.^{5,17} Although it is generally accepted that structural properties of the ACL decrease with advancing age, controversy exists in relation to the effect of age on failure pattern. Some studies have reported a higher incidence of ligament failure in specimens from young donors and a higher incidence of avulsion ACL failure in specimens from older donors,¹⁷ whereas other studies reported that older specimens had a higher incidence of substance failure than younger specimens.⁵ The importance of strain rate with regard to failure mode has also been highlighted, with the tibial avulsion fracture pattern being more frequent in cases of a slow rate and ligament failure being the leading mode in cases of a fast rate.¹⁵ Our strain rate of 1.5 mm/s is within the strain rate range that has been used in similar models,^{5,15-17} and it was selected to allow observation of the sequence of events during uniaxial loading. An evaluation of the correlation of different biological, mechanical, and physical factors with each bundle's performance was beyond of the aims of this study. Furthermore, the number of specimens was relatively small to make safe conclusions.

On the basis of our findings, our future directions include an experimental model to simulate the clinical conditions during ACL rupture. Multiple high-speed video cameras placed at different angles used in real time are needed to evaluate the relation of the rupture pattern with the several combined knee motions that have been considered causative mechanisms of ACL failure.

Our study contains certain limitations. It uses a model of tensile testing that is different from the mechanical condition of the ACL during the proposed injury mechanisms. Numerous combined knee motions have been considered causative mechanisms of ACL rupture.²⁹ ACL rupture can result from either a noncontact event, such as deceleration during a jump landing, a sudden change in direction, or forward running with the knee close to full extension, or a contact event where the knee is forced into valgus collapse.^{30,31} However, this knee motion seems to lead to ACL failure due to the tensile forces applied to it.^{32,33} The abrupt deformation of the ACL due to extension, flexion, rotation, or varus/valgus of the knee in combination with a pre-deformed ACL results in failure of the ACL under tensile conditions.^{32,33} It has been shown that at knee flexion of 15°, the AM and PL have similar in situ force distributions.⁸ Therefore we presume that the rupture occurring would depend on the mechanical properties of the ACL fibers. It was not the goal of this study to reproduce the numerous clinical situations that lead to ACL failure. Our model was used to study the behavior of the fibers

of the ACL under uniaxial loading. The loading axis does not correspond to the force acting on the ACL during a typical knee trauma; therefore, the failure modes of this study will not be observed in patients after typical knee trauma. Furthermore, given the small number of specimens, it is unsafe to make any conclusions concerning the etiology of the 3 different failure patterns shown. The mean age of the specimens was older than the mean age of patients who undergo ACL rupture. Evaluation of the results should take into consideration the potential biological changes to the ACL occurring with advancing age and withdrawals associated with postmortem changes to the specimen.

CONCLUSIONS

The ACL ligament acts as a multifiber construction. In our setting rupture follows 3 specific patterns where a complete or partial tear of the fiber bundles occurs first and the remaining intact fiber bundles have a potential load resistance.

REFERENCES

1. Weber WE, Weber EFM. *Mechanik der menschlichen Gehwerkzeuge*. Göttingen: Der Dietrichschen Buchhandlung, 1836.
2. Girgis FG, Marshall JL, Monajem A. The cruciate ligaments of the knee joint. Anatomical, functional and experimental analysis. *Clin Orthop Relat Res* 1975;216-231.
3. Amis AA, Dawkins GP. Functional anatomy of the anterior cruciate ligament. Fibre bundle actions related to ligament replacements and injuries. *J Bone Joint Surg Br* 1991;73:260-267.
4. Petersen W, Zantop T. Anatomy of the anterior cruciate ligament with regard to its two bundles. *Clin Orthop Relat Res* 2007;454:35-47.
5. Woo SL, Hollis JM, Adams DJ, Lyon RM, Takai S. Tensile properties of the human femur-anterior cruciate ligament-tibia complex. The effects of specimen age and orientation. *Am J Sports Med* 1991;19:217-225.
6. Zantop T, Herbolt M, Raschke MJ, Fu FH, Petersen W. The role of the anteromedial and posterolateral bundles of the anterior cruciate ligament in anterior tibial translation and internal rotation. *Am J Sports Med* 2007;35:223-227.
7. Lipke JM, Janecki CJ, Nelson CL, et al. The role of incompetence of the anterior cruciate and lateral ligaments in anterolateral and anteromedial instability. A biomechanical study of cadaver knees. *J Bone Joint Surg Am* 1981;63:954-960.
8. Gabriel MT, Wong EK, Woo SL, Yagi M, Debski RE. Distribution of in situ forces in the anterior cruciate ligament in response to rotatory loads. *J Orthop Res* 2004;22:85-89.
9. Lo J, Müller O, Wünschel M, Bauer S, Wülker N. Forces in anterior cruciate ligament during simulated weight-bearing flexion with anterior and internal rotational tibial load. *J Biomech* 2008;41:1855-1861.
10. Georgoulis AD, Ristanis S, Chouliaras V, Moraiti C, Stergiou N. Tibial rotation is not restored after ACL reconstruction with a hamstring graft. *Clin Orthop Relat Res* 2007;454:89-94.
11. Chouliaras V, Ristanis S, Moraiti C, Stergiou N, Georgoulis

- AD. Effectiveness of reconstruction of the anterior cruciate ligament with quadrupled hamstrings and bone-patellar tendon-bone autografts: An in vivo study comparing tibial internal-external rotation. *Am J Sports Med* 2007; 35:189-196.
12. Markolf KL, Park S, Jackson SR, McAllister DR. Contributions of the posterolateral bundle of the anterior cruciate ligament to anterior-posterior knee laxity and ligament forces. *Arthroscopy* 2008;24:805-809.
 13. Xerogeanes JW, Takeda Y, Livesay GA, et al. Effect of knee flexion on the in situ force distribution in the human anterior cruciate ligament. *Knee Surg Sports Traumatol Arthrosc* 1995; 3:9-13.
 14. Sakane M, Fox RJ, Woo SL, Livesay GA, Li G, Fu FH. In situ forces in the anterior cruciate ligament and its bundles in response to anterior tibial loads. *J Orthop Res* 1997;15:285-293.
 15. Noyes FR, DeLucas JL, Torvik PJ. Biomechanics of anterior cruciate ligament failure: An analysis of strain-rate sensitivity and mechanisms of failure in primates. *J Bone Joint Surg Am* 1974;56:236-253.
 16. Noyes FR, Torvik PJ, Hyde WB, DeLucas JL. Biomechanics of ligament failure. II. An analysis of immobilization, exercise, and reconditioning effects in primates. *J Bone Joint Surg Am* 1974;56:1406-1418.
 17. Noyes FR, Grood ES. The strength of the anterior cruciate ligament in humans and rhesus monkeys. *J Bone Joint Surg Am* 1976;58:1074-1082.
 18. Zantop T, Brucker PU, Vidal A, Zelle BA, Fu FH. Intraarticular rupture pattern of the ACL. *Clin Orthop Relat Res* 2007; 454:48-53.
 19. Woo SL, Orlando CA, Camp JF, Akeson WH. Effects of postmortem storage by freezing on ligament tensile behavior. *J Biomech* 1986;19:399-404.
 20. Noyes FR. Functional properties of knee ligaments and alterations induced by immobilization: A correlative biomechanical and histological study in primates. *Clin Orthop Relat Res* 1977;210-242.
 21. Kennedy JC, Weinberg HW, Wilson AS. The anatomy and function of the anterior cruciate ligament. As determined by clinical and morphological studies. *J Bone Joint Surg Am* 1974;56:223-235.
 22. Petersen W, Zantop T. Partial rupture of the anterior cruciate ligament. *Arthroscopy* 2006;22:1143-1145.
 23. Odensten M, Lysholm J, Gillquist J. The course of partial anterior cruciate ligament ruptures. *Am J Sports Med* 1985;13: 183-186.
 24. Noyes FR, Mooar LA, Moorman CT III, McGinniss GH. Partial tears of the anterior cruciate ligament. Progression to complete ligament deficiency. *J Bone Joint Surg Br* 1989;71: 825-833.
 25. Chen WT, Shih TT, Tu HY, Chen RC, Shau WY. Partial and complete tear of the anterior cruciate ligament. *Acta Radiol* 2002;43:511-516.
 26. Lawrance JA, Ostlere SJ, Dodd CA. MRI diagnosis of partial tears of the anterior cruciate ligament. *Injury* 1996;27:153-155.
 27. Kelly MA, Flock TJ, Kimmel JA, et al. MR imaging of the knee: Clarification of its role. *Arthroscopy* 1991;7:78-85.
 28. Steckel H, Vadala G, Davis D, Musahl V, Fu FH. 3-T MR imaging of partial ACL tears: A cadaver study. *Knee Surg Sports Traumatol Arthrosc* 2007;15:1066-1071.
 29. Renstrom P, Ljungqvist A, Arendt E, et al. Non-contact ACL injuries in female athletes: An International Olympic Committee current concepts statement. *Br J Sports Med* 2008;42:394-412.
 30. Olsen OE, Myklebust G, Engebretsen L, Bahr R. Injury mechanisms for anterior cruciate ligament injuries in team handball: A systematic video analysis. *Am J Sports Med* 2004;32:1002-1012.
 31. Krosshaug T, Nakamae A, Boden BP, et al. Mechanisms of anterior cruciate ligament injury in basketball: Video analysis of 39 cases. *Am J Sports Med* 2007;35:359-367.
 32. Fuller BB. *Synergetics, explorations in the geometry of thinking*. New York: Macmillan Publishing, 1975.
 33. Levin SM. The importance of soft tissues for structural support of the body. In: Dorman T, ed. *Prolotherapy in the lumbar spine and pelvis*. Philadelphia: Hanley & Belfus, 1995;309-524.